

# On testing in-vacuo dispersion with the most energetic neutrinos: KM3-230213A case study

Giovanni Amelino-Camelia,<sup>1,2</sup> Giacomo D’Amico,<sup>3</sup> Giuseppe Fabiano,<sup>4,5,6</sup>  
Domenico Frattulillo,<sup>2</sup> Giulia Gubitosi,<sup>1,2</sup> Alessandro Moia,<sup>1</sup> and Giacomo Rosati<sup>7,8,9</sup>

<sup>1</sup>*Dipartimento di Fisica Ettore Pancini, Università di Napoli “Federico II”,  
Complesso Univ. Monte S. Angelo, I-80126 Napoli, Italy*

<sup>2</sup>*Istituto Nazionale di Fisica Nucleare, Sezione di Napoli,  
Complesso Univ. Monte S. Angelo, I-80126 Napoli, Italy*

<sup>3</sup>*Institut de Física d’Altes Energies (IFAE), The Barcelona Institute of  
Science and Technology (BIST), E-08193 Bellaterra, (Barcelona), Spain*

<sup>4</sup>*Physics Division, Lawrence Berkeley National Laboratory, Berkeley, CA 94720, USA*

<sup>5</sup>*Department of Physics, University of California, Berkeley, CA 94720, USA*

<sup>6</sup>*Centro Ricerche Enrico Fermi, I-00184 Rome, Italy*

<sup>7</sup>*Dipartimento di Matematica, Università di Cagliari, via Ospedale 72, 09124 Cagliari, Italy*

<sup>8</sup>*Istituto Nazionale di Fisica Nucleare, Sezione di Cagliari,  
Cittadella Universitaria, 09042 Monserrato, Italy*

<sup>9</sup>*Institute for Theoretical Physics, University of Wrocław,  
Pl. Maksa Borna 9, PL-50-204 Wrocław, Poland*

The phenomenology of in-vacuo dispersion, an effect such that quantum properties of spacetime slow down particles proportionally to their energies, has been a very active research area since the advent of the Fermi telescope. One of the assumptions made in this 15-year effort is that the phenomenology of in-vacuo dispersion has a particle-energy sweet spot: the energy of the particle should be large enough to render the analysis immune to source-intrinsic confounding effects but still small enough to facilitate the identification of the source of the particle. We use the gigantic energy of KM3-230213A as an opportunity to challenge this expectation. For a neutrino of a few hundred PeVs a transient source could have been observed at lower energies several years earlier, even assuming the characteristic scale of in-vacuo dispersion to be close to the Planck scale. We report that GRB090401B is in excellent directional agreement with KM3-230213A, and we discuss a strategy of in-vacuo-dispersion analysis suitable for estimating the significance of KM3-230213A as a GRB090401B-neutrino candidate. The  $p$ -value resulting from our analysis (0.015) is not small enough to warrant any excitement, but small enough to establish the point that a handful of such coincidences would be sufficient to meaningfully test in-vacuo dispersion.

Motivated mainly by the fact that it could be caused by quantum properties of spacetime [1–3], in-vacuo dispersion has been studied extensively over the last 15 years, trying to profit from the opportunity provided by modern telescopes like Fermi [4]. The relevant analyses of astrophysical signals are tailored to find the imprint of the in-vacuo-dispersion excess contribution  $\Delta t$  to the travel time of particles

$$\Delta t = D(z) \frac{E}{M_{QG}}, \quad (1)$$

where  $M_{QG}$  is the characteristic scale of in-vacuo dispersion, to be determined experimentally (but expected to be within 1 or 2 orders of magnitude [3] of the Planck scale  $\sim 10^{16}$  TeV) and  $D(z)$  is a function of the redshift  $z$  of the source emitting the particle,

$$D(z) = \int_0^z d\zeta \frac{(1+\zeta)}{H_0 \sqrt{\Omega_\Lambda + (1+\zeta)^3 \Omega_m}}$$

(as usual,  $\Omega_\Lambda$ ,  $H_0$  and  $\Omega_m$  denote, respectively, the cosmological constant, the Hubble parameter and the matter fraction, for which we take the values given in Ref. [5]).

Hundreds of studies focused on the phenomenology of in-vacuo dispersion for photons [3], and recently, as the

public availability of IceCube data increases [6], a few studies have been devoted to in-vacuo dispersion for neutrinos [7–11] (also see the earlier preliminary investigations [12, 13]). The prospect of observing neutrinos from GRBs (gamma-ray bursts) is particularly exciting from the in-vacuo-dispersion perspective, because of the fine time structure and typically large redshift of GRBs [1, 3].

We observe that, as shown in Fig. 1, the estimated direction of the neutrino 230213A (KM3-230213A [14]) is consistent with the direction of the GRB 090401B (GRB090401B [15]). Moreover, the 14-year separation between the two observations would be unsurprising, from the viewpoint of in-vacuo dispersion, considering the remarkably high energy of 230213A. Because of how crowded our Universe is, the burden of proof for arguing a connection between observations separated by 14 years must be very onerous, and indeed we here find (see later) that with presently-available data (and data uncertainties) the case for attributing 230213A to 090401B is not very strong. But what would be needed to make such a type of “GRB-neutrino candidate” statistically significant? Is it at all possible? Would it make a big difference if the direction of 230213A had been determined more sharply? What if at some point we had a few such GRB-neutrino candidates, with large time sep-

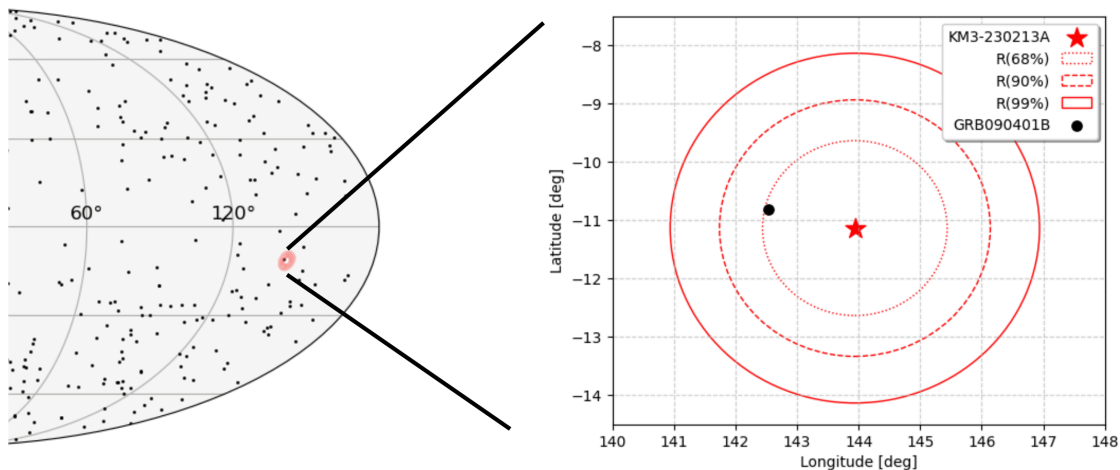


FIG. 1. We here provide an assessment of the directional compatibility between 090401B and 230213A. The dots on the left side reflect the positions of GRBs of known redshift (see Appendix A) and the red circle on the left side reflects the experimental information on the direction of 230213A [14] (the dot inside the red circle is for 090401B). The right side quantifies visually the 090401B-230213A directional compatibility.

aration between observation of the GRB and observation of the ultra-high-energy neutrino?

For the Fermi-telescope phenomenology of in-vacuo dispersion with GRB photons of multi-GeV energies the challenge is complementary: since a Planck-scale estimate of the magnitude of in-vacuo dispersion is in that case of no more than  $\sim 100$  seconds, the identification of the source is straightforward, but then the effect is small enough for its study to be weakened by some known (but poorly understood) source-intrinsic effects which reduce the sensitivity reach of the analysis [3, 4]. For GRB neutrinos the “sweet spot” could be neutrino energies between 100 and 500 TeV [7], for which the magnitude of the effect is big enough to render source-intrinsic effects irrelevant, but still small enough to give realistic chances of source identification.

We here assess the statistical significance of the 090401B-230213A association by relying on a suitable adaptation of the approach developed in Refs. [7, 10, 11], an adaptation which takes into account the challenges faced because of the huge energy (and huge energy uncertainty) of 230213A. The key aspect of our strategy of analysis is that one should quantify in terms of some statistic  $\mathcal{S}_{dir}$  the level of directional agreement between the GRB and the neutrino and quantify in terms of some other statistic  $\mathcal{S}_E$  the level of agreement between the experimental information on the energy of the neutrino and the range of energies that in-vacuo dispersion would predict for such a delayed neutrino observation from a GRB at that redshift. One can then estimate how likely it would be to produce accidentally, if the neutrino was unrelated to the GRB, values of  $\mathcal{S}_{dir}$  and  $\mathcal{S}_E$  as high as those of the studied GRB-neutrino pair.

For what concerns  $\mathcal{S}_{dir}$ , a natural candidate has already been considered in previous multimessenger studies [11, 16]: the statistic  $\mathcal{S}_{dir} = \int P_\nu(\Omega)P_{GRB}(\Omega)d\Omega$ ,

where  $P_\nu(\Omega)$  and  $P_{GRB}(\Omega)$  are the angular distributions of the neutrino and the GRB, respectively, is a good measure of directional compatibility. As visually clear from Fig. 1, we find that the 090401B-230213A association has indeed a rather large  $\mathcal{S}_{dir}$ , equal to 194 (see Appendix B).

There are no previous proposals for the indicator  $\mathcal{S}_E$ . The  $\mathcal{S}_E$  we here propose takes as starting points the redshift  $z$  of the GRB, equal to  $z_{090401B} = 3.1$  in the case of 090401B (see Appendix B), and the  $\Delta t$  between the neutrino observation time and the GRB observation time, which in the case of the 090401B-230213A pair is  $\Delta t_{090401B} = 4.38 \cdot 10^8$  s. In light of the in-vacuo dispersion of Eq. (1), the measured values of  $\Delta t$  and  $z$  allow to convert any chosen value of  $M_{QG}$  into an in-vacuo-dispersion-inferred value of the neutrino energy. The analysis reported in Ref. [10] led to estimating that  $M_{QG}$  could be in the range  $[3.97 \cdot 10^{14}, 9.60 \cdot 10^{14}]$  TeV, using IceCube neutrinos with energy between 60 and 500 TeV and making rather crude assumptions on the redshift of some GRBs whose redshift was not measured. Then in Ref. [11] this same range of values for  $M_{QG}$  was the core ingredient for a rather encouraging analysis (on which we find appropriate to comment in more detail later in this manuscript) restricted to GRBs of known redshift. For the investigation of the 090401B-230213A pair we take once again as reference the range  $[3.97 \cdot 10^{14}, 9.60 \cdot 10^{14}]$  TeV for  $M_{QG}$ . For any given GRB-neutrino pair, using its measured values of  $\Delta t$  and  $z$ , this range of values for  $M_{QG}$  gets converted, on the basis of Eq. (1), into a range  $[E_{min}, E_{max}]$  for the inferred neutrino energy  $E$ . In the case of the 090401B-230213A pair we find  $E_{min} = 119$  PeV and  $E_{max} = 289$  PeV. A good  $\mathcal{S}_E$  statistic should efficaciously characterize the quantitative agreement between this range of (in-vacuo-dispersion-)inferred energies for the neutrino and the experimentally measured range of energies for the neutrino,

which in general will take the form of some energy distribution  $\rho_\nu(E)$ . Our  $\mathcal{S}_E$  indicator is given by

$$\mathcal{S}_E = \int_{E_{min}}^{E_{max}} \frac{\rho_\nu(E)}{E_{max} - E_{min}} dE,$$

which in the case of the 090401B-230213A pair takes the value  $\mathcal{S}_E = 0.00209 \text{ PeV}^{-1}$ , reflecting the fact that, as shown in Fig. 2, a significant portion of  $\rho_{230213A}(E)$  falls within the range [119, 289] PeV.

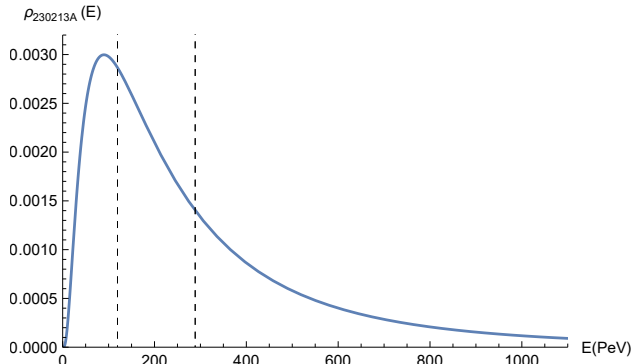


FIG. 2. Here the two vertical lines mark the extrema (119 PeV and 289 PeV) of the range of inferred 230213A energy, obtained using the range of values for  $M_{QG}$  motivated in Ref. [10] and Eq.(1).  $\rho_{230213A}(E)$ , which we used to compute our indicator  $\mathcal{S}_E$ , is a log-normal distribution describing the energy of 230213A, with the properties that its median is 220 PeV, its integral between 110 PeV and 790 PeV is 0.68 and its integral between 72 PeV and 2600 PeV is 0.9 [14].

In order to assess the significance of our findings of  $\mathcal{S}_{dir}$  ( $=194$ ) and  $\mathcal{S}_E$  ( $=0.00209 \text{ PeV}^{-1}$ ), we produce simulated GRB data and use them to establish how frequently values of  $\mathcal{S}_{dir}$  and  $\mathcal{S}_E$  as high as those of the 090401B-230213A pair could be found accidentally, if 090401B and 230213A were actually unconnected. To produce our simulated GRB data we use a rather standard approach [11, 16]: each instance of simulated GRB data is obtained from the actual list of GRBs of known redshift (see Appendix A) by acting on the GRB directions with a random permutation and a random rotation around the Galactic axis. Generating  $10^5$  such instances of simulated data we found that values of  $\mathcal{S}_{dir}$  and  $\mathcal{S}_E$  as high as (or higher than) those of the 090401B-230213A pair occur accidentally only 1.5% of the times, yielding a  $p$ -value of 0.015 (which corresponds to a  $2.4\sigma$  significance in Gaussian statistics).

Having found that the association 090401B-230213A is intriguing but far from conclusive, we can explore possible avenues for a similar GRB-neutrino candidate to be more significant. One realistic avenue is for the uncertainty in the direction of the neutrino to be smaller. It is realistic even for 230213A itself since its present directional uncertainty of  $1.5^\circ$  is dominated by systematics for which the KM3NeT collaboration is planning improvements [14]. As shown in Appendix C, for a GRB-neutrino

pair like 090401B-230213A, but assuming a directional uncertainty of  $0.2^\circ$  for 230213A, an analysis such as ours should achieve a  $p$ -value of  $\sim 0.0002$ .

It is difficult to estimate how frequently we might have observations of neutrinos with energy comparable to 230213A. On the basis of results reported by IceCube [17] one might expect the frequency to be rather low. It is nonetheless worth stressing that if one day we could have a handful of such GRB-neutrino candidates, with individual significance of about 1%, but different (though comparable) energies, then the data could be also used to test [7, 10, 11] the energy-dependence predicted by Eq.(1), strengthening the significance of the analysis. In this respect there is a particularly amusing scenario that can be contemplated: the observation within a few of years of a neutrino with energy 20% or 30% higher than 230213A and direction once again compatible with 090401B.

Even if 230213A remained unique, and if somehow its directional uncertainty was not improved through better control of KM3NeT systematics, the 090401B-230213A candidate pair could still contribute its 1.5% significance to studies of in-vacuo dispersion also involving neutrinos of lower energies. The content of Fig. 3 refers to the 090401B-230213A pair and to four other GRB-neutrino candidates found in Ref. [11]. The study reported in Ref. [11] adopted the same  $M_{QG}$  search window here adopted ( $3.97 \cdot 10^{14} \text{ TeV} < M_{QG} < 9.60 \cdot 10^{14} \text{ TeV}$ , which is reflected in the gray band of Fig. 3) and the four GRB-neutrino candidates of Ref. [11] had an overall significance, from the in-vacuo-dispersion perspective, of 0.6% ( $2.8\sigma$  significance in Gaussian statistics).

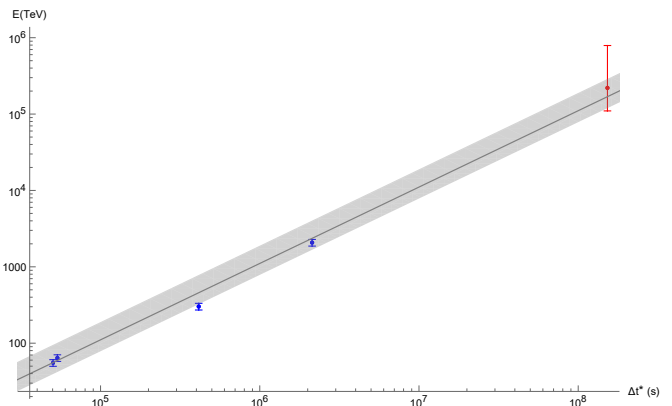


FIG. 3. Here  $\Delta t^*$  is  $\Delta t D(1)/D(z)$  (with  $D(1)$  introduced only for the convenience of having a  $\Delta t^*$  with dimensions of time). According to Eq. (1), for GRB neutrinos there should be a linear relationship between  $E$  and  $\Delta t^*$  (when  $\Delta t^*$  is computed using the redshift  $z$  of the GRB and the  $\Delta t$  between neutrino and GRB). The gray band and the gray line reflect properties of the search window first motivated in Ref. [10]. The highest-energy (red) data point corresponds to the 090401B-230213A pair, while the other four data points represent the four GRB-neutrino candidates found in Ref. [11].

The content of Fig. 3 shows qualitatively a path toward a role for the 090401B-230213A pair in studies of in-vacuo dispersion also involving lower-energy neutrinos. In particular, there is a rather strong consistency, from the in-vacuo-dispersion perspective, between the 090401B-230213A pair and the four GRB-neutrino candidates highlighted in Ref. [11]. Evidently, this consistency could naturally motivate an effort aimed at establishing the combined statistical significance for in-vacuo dispersion of all five GRB-neutrino candidates appearing in Fig. 3. We postpone that assessment to a future study, since we have not yet been able to find a satisfactory way to combine the approaches introduced here and in Ref. [11]: the strategy of analysis here introduced is tailored for the task of assessing the significance of a single GRB-neutrino pair, and is robust enough to handle a large uncertainty in the neutrino energy, while the strategy of analysis of Ref. [11] relies strongly on the energy dependence predicted by Eq. (1), and therefore requires neutrinos whose energy is sharply determined experimentally.

We devote one final remark to the possibility, also much studied in the quantum-gravity literature, that in-vacuo dispersion might be quadratic rather than linear [3]:  $\Delta t = D'(z)E^2/M'_{QG}$ . The directional agreement of the 090401B-230213A pair is still assessed in the same way from the perspective of quadratic in-vacuo-dispersion, and with a single GRB-neutrino candidate one evidently cannot probe the energy dependence of the effect. If however one attributed any relevance to the consistency between 090401B-230213A and the four other GRB-neutrino pairs here discussed in relation to Fig. 3, then only linear dispersion would be viable.

### ACKNOWLEDGMENTS

G.A.-C. and G.G. are grateful for financial support by the Programme STAR Plus, funded by Federico II University and Compagnia di San Paolo, and by the MIUR, PRIN 2017 grant 20179ZF5KS. G.R.'s work on this project was supported by the National Science Centre grant 2019/33/B/ST2/00050. G.D.'s work on this project was supported by the Beatriu de Pinós programme (BP 2023). G.F.'s work on this project was supported by "The Foundation Blanceflor". This work also falls within the scopes of the COST Action CA23130 "Bridging high and low energies in search of quantum gravity" and the COST Action CA18108 "Quantum Gravity phenomenology in the Multi-Messenger era".

### Appendix A: Known-redshift GRB data

In Appendix A of Ref. [11] we reported a table of GRBs whose redshift has been measured, collecting and cross-checking information from different publicly available catalogues, as well as fixing their occasional inad-

equacies referring to the original GCNs and other publications on the relevant GRBs. That effort focused on the GRBs observed in the years relevant for the analysis reported in Ref. [11]. To obtain Fig. 4 and the table reported in this appendix we adopted the same criteria and approach used for (and described in detail in) Appendix A of Ref. [11] and extended the list of known-redshift GRBs all the way back to 1997. All directions in the table have an uncertainty of no more than  $0.001^\circ$ , which can be safely neglected when computing our indicator  $\mathcal{S}_{dir}$  for pairs composed by 230213A and one of the GRBs here listed.

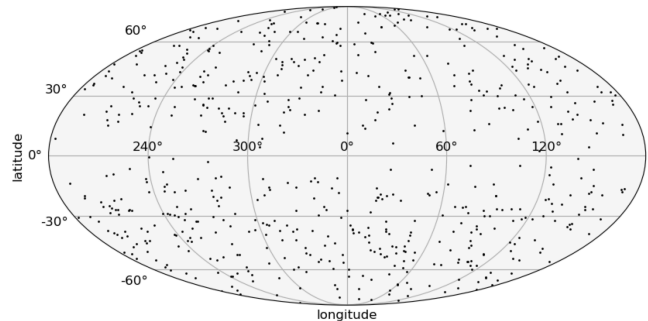


FIG. 4. Mollweide projection of the full sky in galactic coordinates showing the known-redshift GRBs reported in Table I.

TABLE I: List of GRBs with measured redshift

Name	RA ( $^\circ$ )	decl ( $^\circ$ )	TT (MJD)	$z$
GRB221226B	22.909	-41.527	59939.945	2.694
GRB221110A	29.100	-27.294	59893.103	4.06
GRB221009A	288.264	19.773	59861.553	0.151
GRB221006A	337.246	15.714	59858.04	0.731
GRB220813A	81.532	-33.016	59804.808	0.82
GRB220627A	201.369	-32.426	59757.89	3.084
GRB220611A	66.515	-37.260	59741.751	2.3608
GRB220527A	323.528	-14.972	59726.387	0.857
GRB220521A	275.230	10.372	59720.972	5.6
GRB220219B	240.914	31.234	59629.394	0.293
GRB220117A	91.572	-28.437	59596.68	4.961
GRB220107A	169.807	34.171	59586.615	1.246
GRB220101A	1.353	31.769	59580.215	4.618
GRB211227A	132.149	-2.735	59575.981	0.228
GRB211211A	212.292	27.889	59559.549	0.073
GRB211207A	149.624	-24.359	59555.87	2.272
GRB211024B	154.713	24.568	59511.931	1.1137
GRB211023B	170.310	39.136	59510.879	0.862
GRB211023A	73.154	85.324	59510.546	0.39
GRB210919A	80.254	1.312	59476.02	0.2411
GRB210905A	309.048	-44.440	59462.009	6.318
GRB210822A	304.438	5.283	59448.388	1.736
GRB210731A	300.305	-28.061	59426.931	1.2525
GRB210722A	27.030	-6.347	59417.871	1.145
GRB210702A	168.578	-36.747	59397.797	1.16
GRB210619B	319.718	33.850	59385.	1.937
GRB210610B	243.918	14.399	59375.827	1.13
GRB210610A	204.282	14.465	59375.628	3.54
GRB210517A	358.224	-39.102	59351.228	2.486

Name	RA (°)	decl (°)	TT (MJD)	z
GRB210504A	222.392	-30.534	59338.58	2.077
GRB210420B	254.325	42.570	59324.774	1.4
GRB210411C	296.612	-39.398	59315.629	2.826
GRB210323A	317.947	25.369	59296.918	0.733
GRB210321A	87.895	70.130	59294.301	1.487
GRB210312B	155.814	76.869	59285.87	1.069
GRB210222B	154.606	-14.932	59267.943	2.198
GRB210210A	262.771	14.663	59255.084	0.715
GRB210204A	117.081	11.410	59249.27	0.876
GRB210116A	123.814	-5.867	59230.246	2.514
GRB210112A	219.006	33.054	59226.067	2
GRB210104A	103.772	64.676	59218.477	0.46
GRB201221D	171.059	42.144	59204.963	1.046
GRB201221A	214.480	-45.416	59204.298	5.7
GRB201216C	16.370	16.516	59199.963	1.1
GRB201104B	5.215	7.842	59157.732	1.954
GRB201103B	42.185	12.137	59156.755	1.105
GRB201024A	125.952	3.354	59146.117	0.999
GRB201021C	12.529	-55.866	59143.852	1.07
GRB201020B	75.470	77.068	59142.732	0.804
GRB201020A	261.228	31.428	59142.241	2.903
GRB201015A	354.319	53.416	59137.952	0.426
GRB201014A	20.796	27.660	59136.95	4.56
GRB200829A	251.205	72.329	59090.582	1.25
GRB200826A	6.786	34.027	59087.187	0.7481
GRB200613A	153.042	45.754	59013.229	1.2268
GRB200524A	213.043	60.905	58993.211	1.256
GRB200522A	5.682	-0.283	58991.487	0.554
GRB200411A	47.664	-52.318	58950.187	0.7
GRB200219A	342.638	-59.120	58898.317	0.48
GRB200205B	107.788	-56.488	58884.807	1.465
GRB191221B	154.830	-38.158	58838.861	1.148
GRB191031D	283.289	47.644	58787.891	0.5
GRB191019A	340.025	-17.328	58775.634	0.248
GRB191011A	44.728	-27.845	58767.192	1.722
GRB191004B	49.205	-39.634	58760.898	3.503
GRB190919B	311.877	-44.695	58745.991	3.225
GRB190829A	44.544	-8.958	58724.83	0.0785
GRB190719C	240.207	13.000	58683.624	2.469
GRB190627A	244.828	-5.289	58661.471	1.942
GRB190613A	182.529	67.235	58647.172	2.78
GRB190324A	49.616	-47.215	58566.947	1.1715
GRB190114C	54.505	-26.946	58497.873	0.42
GRB190114A	65.544	2.192	58497.133	3.3765
GRB190106A	29.880	23.846	58489.566	1.859
GRB181201A	319.297	-12.631	58453.11	0.45
GRB181123B	184.367	14.598	58445.231	1.754
GRB181110A	302.318	-36.897	58432.364	1.505
GRB181020A	13.982	-47.381	58411.792	2.938
GRB181010A	52.570	-23.038	58401.247	1.39
GRB180914B	332.356	25.062	58375.766	1.096
GRB180805B	25.782	-17.494	58335.543	0.661
GRB180728A	253.565	-54.044	58327.728	0.117
GRB180727A	346.666	-63.052	58326.594	2
GRB180720B	0.529	-2.919	58319.598	0.654
GRB180703A	6.468	-67.179	58302.876	0.6678
GRB180624A	318.098	-2.338	58293.576	2.855
GRB180620B	357.521	-57.962	58289.66	1.1175
GRB180618A	169.941	73.837	58287.03	0.544
GRB180510B	77.969	-62.324	58248.844	1.305
GRB180418A	170.122	24.933	58226.281	1.55

Name	RA (°)	decl (°)	TT (MJD)	z
GRB180404A	83.548	-37.168	58212.032	1.
GRB180329B	82.904	-23.690	58206.589	1.998
GRB180325A	157.428	24.464	58202.078	2.25
GRB180314A	99.265	-24.496	58191.03	1.445
GRB180205A	126.820	11.542	58154.184	1.409
GRB180115A	12.039	-15.630	58133.178	2.487
GRB171222A	148.278	35.627	58109.684	2.409
GRB171205A	167.415	-12.588	58092.306	0.0368
GRB171020A	39.248	15.204	58046.963	1.87
GRB171010A	66.581	-10.463	58036.792	0.3293
GRB170903A	254.526	34.979	57999.534	0.886
GRB170817A	197.450	-23.381	57982.529	0.0093
GRB170728B	237.981	70.122	57962.961	1.27
GRB170728A	58.888	12.182	57962.287	1.49
GRB170714A	34.350	1.991	57948.518	0.793
GRB170705A	191.704	18.307	57939.115	2.01
GRB170607A	7.366	9.243	57911.971	0.557
GRB170604A	342.656	-15.412	57908.798	1.329
GRB170531B	286.884	-16.418	57904.918	2.366
GRB170519A	163.427	25.374	57892.215	0.818
GRB170428A	330.078	26.916	57871.384	0.454
GRB170405A	219.828	-25.243	57848.777	3.51
GRB170214A	256.341	-1.888	57798.649	2.53
GRB170202A	152.514	5.012	57786.769	3.645
GRB170127B	19.977	-30.358	57780.634	2.2
GRB170113A	61.733	-71.943	57766.42	1.968
GRB161219B	91.714	-26.792	57741.784	0.1475
GRB161129A	316.228	32.135	57721.3	0.645
GRB161117A	322.052	-29.614	57709.066	1.549
GRB161108A	180.788	24.868	57700.148	1.159
GRB161104A	77.894	-51.460	57696.404	0.79
GRB161023A	311.022	-47.663	57684.944	2.708
GRB161017A	142.769	43.127	57678.744	2.013
GRB161014A	332.648	7.469	57675.522	2.823
GRB161001A	71.920	-57.261	57662.045	0.67
GRB160821B	279.977	62.392	57621.937	0.16
GRB160804A	221.630	9.999	57604.064	0.736
GRB160629A	4.863	76.967	57568.93	3.332
GRB160625B	308.598	6.919	57564.945	1.406
GRB160624A	330.193	29.644	57563.477	0.483
GRB160623A	315.298	42.221	57562.208	0.367
GRB160509A	311.754	76.108	57517.374	1.17
GRB160425A	280.327	-54.360	57503.977	0.555
GRB160410A	150.685	3.478	57488.215	1.717
GRB160408A	122.625	71.128	57486.268	1.9
GRB160327A	146.702	54.013	57474.386	4.99
GRB160314A	112.790	17.000	57461.481	0.726
GRB160303A	168.701	22.742	57450.455	1
GRB160228A	107.316	26.932	57446.732	1.64
GRB160227A	194.808	78.679	57445.814	2.38
GRB160203A	161.951	-24.789	57421.092	3.52
GRB160131A	78.168	-7.050	57418.348	0.971
GRB160121A	109.088	-23.592	57408.577	1.96
GRB160117B	132.195	-16.367	57404.583	0.87
GRB151229A	329.370	-20.732	57385.285	1.4
GRB151215A	93.584	35.516	57371.126	2.59
GRB151112A	2.054	-61.663	57338.573	4.1
GRB151111A	56.845	-44.161	57337.356	3.5
GRB151031A	83.196	-39.122	57326.243	1.167
GRB151029A	38.528	-35.386	57324.326	1.423
GRB151027B	76.220	-6.450	57322.945	4.063

Name	RA (°)	decl (°)	TT (MJD)	z
GRB151027A	272.487	61.353	57322.166	0.81
GRB151021A	337.644	-33.197	57316.062	2.33
GRB150915A	319.658	-34.914	57280.888	1.968
GRB150910A	5.667	33.473	57275.378	1.359
GRB150831A	221.024	-25.635	57265.44	1.18
GRB150821A	341.913	-57.894	57255.406	0.755
GRB150818A	230.356	68.342	57252.484	0.282
GRB150728A	292.229	33.916	57231.536	0.46
GRB150727A	203.969	-18.325	57230.793	0.313
GRB150616A	314.717	-53.394	57189.951	1.188
GRB150518A	234.201	16.330	57160.904	0.256
GRB150514A	74.876	-60.968	57156.774	0.807
GRB150424A	152.306	-26.631	57136.321	1
GRB150423A	221.579	12.284	57135.269	1.394
GRB150413A	190.425	71.841	57125.58	3.139
GRB150403A	311.505	-62.711	57115.913	2.06
GRB150323A	128.178	45.465	57104.118	0.593
GRB150314A	126.670	63.834	57095.205	1.758
GRB150301B	89.166	-57.970	57082.818	1.5169
GRB150206A	10.074	-63.182	57059.604	2.087
GRB150120B	39.291	8.078	57042.307	3.5
GRB150120A	10.319	33.995	57042.123	0.46
GRB150101B	188.020	-10.934	57023.641	0.134
GRB141225A	138.779	33.792	57016.959	0.915
GRB141221A	198.287	8.205	57012.338	1.452
GRB141220A	195.066	32.146	57011.252	1.3195
GRB141212A	39.125	18.147	57003.51	0.596
GRB141121A	122.669	22.217	56982.15	1.47
GRB141109A	144.531	-0.608	56970.243	2.993
GRB141028A	322.602	-0.231	56958.455	2.33
GRB141026A	44.084	26.928	56956.109	3.35
GRB141004A	76.734	12.820	56934.973	0.571
GRB140930B	6.348	24.295	56930.821	1.465
GRB140907A	48.146	46.605	56907.672	1.21
GRB140903A	238.014	27.603	56903.625	0.351
GRB140808A	221.222	49.215	56877.037	3.29
GRB140801A	44.069	30.938	56870.792	1.32
GRB140713A	281.106	59.634	56851.78	0.935
GRB140710A	41.068	35.499	56848.428	0.558
GRB140703A	12.996	45.102	56841.026	3.14
GRB140629A	248.977	41.877	56837.595	2.275
GRB140623A	225.473	81.191	56831.223	1.92
GRB140622A	317.173	-14.419	56830.4	0.959
GRB140620A	281.871	49.731	56828.219	2.04
GRB140614A	231.169	-79.129	56822.045	4.233
GRB140606B	328.125	32.015	56814.133	0.384
GRB140518A	227.252	42.418	56795.387	4.707
GRB140515A	186.064	15.105	56792.384	6.32
GRB140512A	289.370	-15.094	56789.814	0.725
GRB140509A	46.594	-62.639	56786.099	2.4
GRB140508A	255.466	46.780	56785.128	1.0285
GRB140506A	276.775	-55.636	56783.88	0.889
GRB140430A	102.936	23.024	56777.857	1.6
GRB140428A	194.368	28.385	56775.945	4.7
GRB140423A	197.286	49.842	56770.355	3.26
GRB140419A	126.990	46.240	56766.171	3.956
GRB140331A	134.864	2.717	56747.243	1
GRB140318A	184.089	20.209	56734.006	1.02
GRB140311A	209.305	0.642	56727.879	4.952
GRB140304A	30.643	33.474	56720.557	5.283
GRB140301A	69.558	-34.257	56717.642	1.416

Name	RA (°)	decl (°)	TT (MJD)	z
GRB140226A	221.492	14.993	56714.419	1.98
GRB140213A	105.155	-73.137	56701.807	1.2076
GRB140206A	145.334	66.761	56694.304	2.73
GRB140129B	326.757	26.206	56686.536	0.43
GRB140114A	188.522	27.951	56671.498	3.
GRB131231A	10.590	-1.653	56657.198	0.642
GRB131229A	85.232	-4.396	56655.277	1
GRB131227A	67.378	28.883	56653.198	5.3
GRB131117A	332.331	-31.762	56613.024	4.042
GRB131108A	156.502	9.662	56604.862	2.4
GRB131105A	70.967	-62.995	56601.087	1.686
GRB131103A	348.919	-44.640	56599.922	0.599
GRB131030A	345.067	-5.368	56595.872	1.293
GRB131011A	32.526	-4.411	56576.741	1.874
GRB131004A	296.113	-2.958	56569.904	0.717
GRB130925A	41.179	-26.153	56560.164	0.347
GRB130907A	215.892	45.608	56542.902	1.238
GRB130831A	358.624	29.430	56535.545	0.4791
GRB130822A	27.922	-3.208	56526.663	0.154
GRB130716A	179.574	63.053	56489.442	2.2
GRB130702A	217.312	15.774	56475.004	0.145
GRB130701A	357.229	36.100	56474.179	1.155
GRB130615A	274.829	-68.161	56458.406	2.9
GRB130612A	259.794	16.720	56455.141	2.006
GRB130610A	224.420	28.207	56453.133	2.092
GRB130606A	249.396	29.796	56449.878	5.91
GRB130604A	250.187	68.226	56447.288	1.06
GRB130603B	172.201	17.071	56446.659	0.356
GRB130528A	139.505	87.301	56440.695	1.25
GRB130518A	355.668	47.465	56430.58	2.489
GRB130515A	283.440	-54.279	56427.056	0.8
GRB130514A	296.283	-7.976	56426.301	3.6
GRB130511A	196.646	18.710	56423.48	1.3033
GRB130505A	137.061	17.485	56417.349	2.27
GRB130427B	314.898	-22.546	56409.556	2.78
GRB130427A	173.137	27.699	56409.324	0.34
GRB130420A	196.106	59.424	56402.311	1.297
GRB130418A	149.037	13.667	56400.792	1.218
GRB130408A	134.405	-32.361	56390.911	3.758
GRB130215A	43.503	13.395	56338.063	0.597
GRB130131B	173.956	15.038	56323.799	2.539
GRB130131A	171.127	48.076	56323.581	1.55
GRB121229A	190.101	-50.594	56290.209	2.707
GRB121226A	168.642	-30.406	56287.798	1.37
GRB121217A	153.710	-62.351	56278.303	3.1
GRB121211A	195.533	30.148	56272.574	1.023
GRB121209A	326.787	-8.235	56270.916	2.1
GRB121201A	13.467	-42.943	56262.518	3.385
GRB121128A	300.600	54.300	56259.212	2.2
GRB121123A	307.318	-11.860	56254.419	2.7
GRB121027A	63.598	-58.830	56227.314	1.773
GRB121024A	70.472	-12.291	56224.122	2.298
GRB120923A	303.795	6.221	56193.22	7.8
GRB120922A	234.748	-20.182	56192.938	3.1
GRB120909A	275.736	-59.449	56179.07	3.93
GRB120907A	74.750	-9.315	56177.017	0.97
GRB120815A	273.958	-52.131	56154.093	2.358
GRB120811C	199.683	62.301	56150.649	2.671
GRB120805A	216.538	5.825	56144.895	3.1
GRB120804A	233.948	-28.782	56143.038	1.05
GRB120802A	44.843	13.768	56141.334	3.796

Name	RA (°)	decl (°)	TT (MJD)	z
GRB120729A	13.074	49.940	56137.456	0.8
GRB120724A	245.181	3.508	56132.277	1.48
GRB120722A	230.497	13.251	56130.537	0.9586
GRB120716A	313.051	9.599	56124.712	2.486
GRB120714B	355.409	-46.184	56122.888	0.3984
GRB120712A	169.588	-20.034	56120.571	4.17
GRB120711A	94.678	-70.999	56119.114	1.405
GRB120630A	352.296	42.556	56108.971	0.6
GRB120624B	170.885	8.929	56102.93	2.1974
GRB120521C	214.286	42.145	56068.974	6.
GRB120422A	136.910	14.019	56039.3	0.283
GRB120404A	235.010	12.885	56021.535	2.876
GRB120401A	58.082	-17.636	56018.225	4.5
GRB120327A	246.864	-29.415	56013.122	2.8115
GRB120326A	273.905	69.260	56012.056	1.798
GRB120311A	273.092	14.296	55997.232	0.35
GRB120305A	47.536	28.492	55991.818	0.225
GRB120224A	40.942	-17.761	55981.194	1.1
GRB120211A	87.754	-24.775	55968.499	2.4
GRB120119A	120.029	-9.082	55945.17	1.728
GRB120118B	124.871	-7.185	55944.709	2.943
GRB111229A	76.287	-84.711	55924.943	1.3805
GRB111228A	150.067	18.298	55923.656	0.714
GRB111225A	13.155	51.572	55920.16	0.297
GRB111215A	349.556	32.494	55910.586	2.06
GRB111211A	153.090	11.208	55906.929	0.478
GRB111209A	14.344	-46.801	55904.3	0.677
GRB111129A	307.434	-52.713	55894.679	1.0796
GRB111123A	154.846	-20.645	55888.759	3.1516
GRB111117A	12.693	23.011	55882.51	2.211
GRB111107A	129.478	-66.520	55872.035	2.893
GRB111008A	60.451	-32.709	55842.926	5.
GRB111005A	223.282	-19.737	55839.337	0.0131
GRB110918A	32.539	-27.105	55822.894	0.982
GRB110818A	317.337	-63.981	55791.86	3.36
GRB110808A	57.268	-44.194	55781.263	1.348
GRB110801A	89.437	80.956	55774.826	1.858
GRB110731A	280.504	-28.537	55773.465	2.83
GRB110721A	333.659	-38.593	55763.2	0.382
GRB110715A	237.684	-46.235	55757.551	0.82
GRB110709B	164.654	-23.455	55751.898	2.109
GRB110503A	132.776	52.208	55684.733	1.613
GRB110422A	112.046	75.107	55673.654	1.77
GRB110402A	197.402	61.253	55653.009	0.854
GRB110213B	41.756	1.146	55605.605	1.083
GRB110213A	42.964	49.273	55605.22	1.46
GRB110205A	164.630	67.525	55597.085	2.22
GRB110128A	193.896	28.065	55589.073	2.339
GRB110106B	134.154	47.003	55567.893	0.618
GRB110106A	79.306	64.174	55567.643	0.093
GRB101225A	0.198	44.600	55555.776	0.847
GRB101224A	285.924	45.714	55554.227	0.4536
GRB101219B	12.231	-34.566	55549.686	0.5519
GRB101219A	74.585	-2.540	55549.105	0.718
GRB101213A	241.314	21.897	55543.451	0.414
GRB100906A	28.684	55.630	55445.576	1.727
GRB100905A	31.550	14.930	55444.631	7.9
GRB100902A	48.629	30.979	55441.814	4.5
GRB100901A	27.264	22.759	55440.565	1.408
GRB100816A	351.740	26.578	55424.026	0.8035
GRB100814A	22.473	-17.995	55422.16	1.44

Name	RA (°)	decl (°)	TT (MJD)	z
GRB100805A	299.876	52.628	55413.186	1.85
GRB100728B	44.056	0.281	55405.439	2.106
GRB100728A	88.758	-15.256	55405.095	1.567
GRB100724A	194.543	-11.103	55401.029	1.288
GRB100704A	133.642	-24.203	55381.149	3.6
GRB100628A	225.973	-31.664	55375.345	0.102
GRB100625A	15.796	-39.088	55372.773	0.452
GRB100621A	315.305	-51.106	55368.127	0.542
GRB100615A	177.205	-19.481	55362.083	1.398
GRB100606A	350.627	-66.241	55353.8	1.5545
GRB100518A	304.789	-24.554	55334.482	4.
GRB100513A	169.612	3.628	55329.088	4.772
GRB100508A	76.246	-20.711	55324.389	0.5201
GRB100425A	299.196	-26.431	55311.119	1.755
GRB100424A	209.448	1.538	55310.689	2.465
GRB100418A	256.362	11.462	55304.882	0.6235
GRB100414A	192.112	8.693	55300.097	1.368
GRB100413A	266.221	15.834	55299.732	3.9
GRB100316D	107.628	-56.256	55271.531	0.059
GRB100316B	163.488	-45.473	55271.334	1.18
GRB100316A	251.978	71.827	55271.099	3.155
GRB100302A	195.516	74.590	55257.829	4.813
GRB100219A	154.202	-12.566	55246.636	4.6667
GRB100216A	154.251	35.522	55243.422	0.038
GRB100213B	124.282	43.448	55240.957	0.604
GRB100206A	47.163	13.157	55233.563	0.41
GRB100117A	11.269	-1.595	55213.879	0.92
GRB091208B	29.392	16.890	55173.41	1.063
GRB091127	36.583	-18.952	55162.976	0.49
GRB091117A	30.972	-16.975	55152.739	0.096
GRB091109	309.258	-44.158	55144.207	3.076
GRB091029	60.178	-55.956	55133.162	2.752
GRB091024	339.248	56.890	55128.372	1.092
GRB091020	175.730	50.978	55124.9	1.71
GRB091018	32.186	-57.548	55122.867	0.971
GRB091003	251.520	36.625	55107.191	0.8969
GRB090927	343.972	-70.980	55101.422	1.37
GRB090926B	46.308	-39.006	55100.914	1.24
GRB090926A	353.400	-66.324	55100.181	2.1062
GRB090902B	264.939	27.324	55076.462	1.822
GRB090814	239.610	25.631	55057.036	0.696
GRB090812	353.202	-10.605	55055.251	2.452
GRB090809	328.680	-0.084	55052.73	2.737
GRB090726	248.680	72.884	55038.946	2.71
GRB090715B	251.340	44.839	55027.877	3.
GRB090709A	289.927	60.728	55021.319	1.8
GRB090618	293.994	78.357	55000.353	0.54
GRB090530	179.419	26.594	54981.138	1.266
GRB090529	212.469	24.459	54980.592	2.625
GRB090519	142.279	0.180	54970.881	3.875
GRB090516	138.260	-11.854	54967.352	4.1045
GRB090510	333.552	-26.583	54961.016	0.903
GRB090429B	210.667	32.170	54950.229	9.4
GRB090426	189.075	32.986	54947.534	2.609
GRB090424	189.521	16.838	54945.589	0.544
GRB090423	148.889	18.149	54944.33	8.26
GRB090418	269.313	33.406	54939.464	1.608
GRB090417B	209.694	47.018	54938.639	0.345
GRB090407	68.980	-12.679	54928.436	1.4485
GRB090404	239.240	35.516	54925.664	3
GRB090401B	95.088	-8.972	54922.358	3.1

Name	RA (°)	decl (°)	TT (MJD)	z
GRB090328	90.665	-41.882	54918.401	0.736
GRB090323	190.710	17.053	54913.002	3.57
GRB090313	198.401	8.097	54903.379	3.375
GRB090205	220.911	-27.853	54867.961	4.6497
GRB090201	92.052	-46.590	54863.741	2.1
GRB090113	32.057	33.428	54844.778	1.7493
GRB090102	128.244	33.114	54833.122	1.547
GRB081230	37.331	-25.148	54830.858	2
GRB081228	39.462	30.853	54828.054	3.44
GRB081222	22.740	-34.095	54822.204	2.77
GRB081221	15.793	-24.548	54821.681	2.26
GRB081211B	168.265	53.830	54811.26	0.216
GRB081210	70.484	-11.257	54810.847	2.0631
GRB081203	233.032	63.521	54803.577	2.05
GRB081121	89.276	-60.603	54791.858	2.512
GRB081118	82.592	-43.301	54788.623	2.58
GRB081109	330.790	-54.711	54779.293	0.9787
GRB081029	346.772	-68.156	54768.072	3.8479
GRB081028	121.895	2.308	54767.017	3.038
GRB081008	279.958	-57.431	54747.832	1.967
GRB081007	339.960	-40.147	54746.224	0.5295
GRB080928	95.070	-55.200	54737.626	1.692
GRB080916C	119.847	-56.638	54725.009	4.35
GRB080916	336.276	-57.023	54725.406	0.689
GRB080913	65.728	-25.130	54722.283	6.5675
GRB080906	228.044	-80.518	54715.565	2.
GRB080905B	301.741	-62.563	54714.705	2.374
GRB080905	287.674	-18.880	54714.499	0.1218
GRB080825B	209.201	-68.955	54703.741	4.3
GRB080810	356.793	0.320	54688.549	3.35
GRB080805	314.223	-62.445	54683.321	1.505
GRB080804	328.668	-53.185	54682.972	2.2045
GRB080721	224.483	-11.724	54668.434	2.5987
GRB080710	8.274	19.502	54657.301	0.845
GRB080707	32.618	33.109	54654.353	1.23
GRB080607	194.947	15.920	54624.255	3.036
GRB080605	262.125	4.016	54622.992	1.6398
GRB080604	236.965	20.558	54621.31	1.416
GRB080603B	176.532	68.061	54620.818	2.69
GRB080603	279.409	62.744	54620.471	1.688
GRB080602	19.176	-9.232	54619.063	1.8204
GRB080520	280.193	-54.992	54606.931	1.545
GRB080517	102.242	50.735	54603.891	0.089
GRB080516	120.642	-26.160	54602.012	3.2
GRB080515	3.163	32.578	54601.251	2.47
GRB080514B	322.845	0.708	54600.414	1.8
GRB080430	165.311	51.686	54586.828	0.767
GRB080413B	326.144	-19.981	54569.369	1.1
GRB080413	287.299	-27.678	54569.121	2.433
GRB080411	37.980	-71.302	54567.886	1.03
GRB080330	169.269	30.623	54555.154	1.51
GRB080325	277.893	36.524	54550.173	1.78
GRB080319C	258.981	55.392	54544.518	1.95
GRB080319B	217.921	36.302	54544.259	0.937
GRB080319	206.333	44.080	54544.24	2.0265
GRB080310	220.058	-0.175	54535.36	2.42
GRB080210	251.267	13.827	54506.326	2.641
GRB080207	207.512	7.502	54503.896	2.0858
GRB080205	98.253	62.792	54501.33	2.72
GRB080129	105.284	-7.846	54494.255	4.349
GRB080123	338.943	-64.901	54488.182	0.495

Name	RA (°)	decl (°)	TT (MJD)	z
GRB071227	58.130	-55.984	54461.843	0.383
GRB071122	276.605	47.075	54426.058	1.14
GRB071117	335.044	-63.443	54421.618	1.331
GRB071112C	39.212	28.371	54416.773	0.823
GRB071031	6.405	-58.060	54404.046	2.692
GRB071028B	354.163	-31.621	54401.114	0.94
GRB071025	355.071	31.778	54398.173	5.2
GRB071021	340.643	23.718	54394.404	2.452
GRB071020	119.665	32.861	54393.293	2.145
GRB071010B	150.539	45.730	54383.865	0.947
GRB071010	288.060	-32.402	54383.154	0.98
GRB071003	301.851	10.947	54376.32	1.60435
GRB070810	189.963	10.751	54322.092	2.17
GRB070809	203.770	-22.142	54321.807	0.2187
GRB070802	36.899	-55.528	54314.297	2.45
GRB070724	27.808	-18.594	54305.454	0.457
GRB070721B	33.137	-2.195	54302.44	3.626
GRB070714B	57.843	28.298	54295.208	0.92
GRB070714	42.930	30.243	54295.139	1.58
GRB070612	121.369	37.269	54263.11	0.617
GRB070611	1.992	-29.756	54262.081	2.04
GRB070529	283.742	20.659	54249.534	2.4996
GRB070521	242.661	30.256	54241.286	2.0865
GRB070508	312.799	-78.385	54228.179	0.82
GRB070506	347.218	10.722	54226.233	2.31
GRB070429B	328.015	-38.829	54219.131	0.904
GRB070419B	315.707	-31.264	54209.447	1.9591
GRB070419	182.745	39.925	54209.416	0.97
GRB070411	107.333	1.064	54201.842	2.954
GRB070328	65.115	-34.067	54187.162	2.0627
GRB070318	48.487	-42.946	54177.312	0.836
GRB070306	148.097	10.482	54165.695	1.4965
GRB070224	179.027	-13.330	54155.853	1.9922
GRB070223	153.452	43.134	54154.052	1.6295
GRB070208	197.886	61.965	54139.382	1.165
GRB070129	37.004	11.684	54129.983	2.3384
GRB070125	117.824	31.151	54125.306	1.547
GRB070110	0.913	-52.974	54110.307	2.352
GRB070103	352.558	26.876	54103.866	2.6208
GRB061222B	105.353	-25.860	54091.174	3.355
GRB061222	358.264	46.533	54091.145	2.088
GRB061217	160.413	-21.124	54086.153	0.827
GRB061210	144.522	15.621	54079.514	0.4097
GRB061202	105.525	-74.698	54071.341	2.2543
GRB061201	332.134	-74.580	54070.666	0.111
GRB061126	86.602	64.211	54065.367	1.1588
GRB061121	147.227	-13.195	54060.641	1.314
GRB061110B	323.919	6.876	54049.916	3.44
GRB061110	336.291	-2.258	54049.491	0.758
GRB061021	145.150	-21.952	54029.652	0.3463
GRB061007	46.332	-50.501	54015.422	1.261
GRB061006	111.031	-79.199	54014.699	0.4377
GRB060927	329.550	5.364	54005.589	5.535
GRB060926	263.932	13.038	54004.7	3.204
GRB060923B	238.195	-30.904	54001.485	1.5094
GRB060912	5.284	20.972	53990.58	0.937
GRB060908	31.826	0.342	53986.373	1.8836
GRB060906	40.754	30.362	53984.356	3.6855
GRB060904B	58.211	-0.725	53982.105	0.703
GRB060814	221.339	20.586	53961.96	1.3815
GRB060805	220.931	12.586	53952.2	2.3633



Name	RA (°)	decl (°)	TT (MJD)	z
GRB060801	213.006	16.982	53948.511	1.131
GRB060729	95.382	-62.370	53945.8	0.54
GRB060719	18.432	-48.381	53935.285	1.532
GRB060714	227.860	-6.566	53930.633	2.7105
GRB060708	7.808	-33.759	53924.511	2.11
GRB060707	357.080	-17.905	53923.896	3.4275
GRB060614	320.884	-53.027	53900.53	0.1275
GRB060607	329.710	-22.496	53893.217	3.0785
GRB060605	322.156	-6.059	53891.761	3.79
GRB060604	337.229	-10.916	53890.763	2.1357
GRB060526	232.826	0.285	53881.686	3.2155
GRB060522	322.937	2.886	53877.091	5.11
GRB060512	195.774	41.191	53867.968	1.2714
GRB060510B	239.122	78.570	53865.349	4.92
GRB060510	95.867	-1.163	53865.322	1.2
GRB060505	331.764	-27.815	53860.275	0.089
GRB060502B	278.938	52.632	53857.725	0.287
GRB060502	240.927	66.601	53857.127	1.51
GRB060418	236.428	-3.639	53843.129	1.4895
GRB060319	176.388	60.011	53813.039	1.172
GRB060306	41.095	-2.148	53800.034	1.559
GRB060223	55.206	-17.130	53789.253	4.41
GRB060218	50.416	16.867	53784.149	0.0331
GRB060210	57.739	27.026	53776.208	3.91
GRB060206	202.931	35.051	53772.199	4.0465
GRB060204B	211.812	27.677	53770.607	2.3393
GRB060202	35.846	38.384	53768.362	0.783
GRB060124	77.108	69.741	53759.663	2.298
GRB060123	179.700	45.514	53758.932	0.8295
GRB060121	137.466	45.663	53756.933	4.6
GRB060116	84.693	-5.437	53751.359	6.6
GRB060115	54.035	17.345	53750.547	3.53
GRB060111	276.205	37.604	53746.183	2.32
GRB060108	147.009	31.919	53743.611	2.03
GRB051227	125.241	31.925	53731.755	0.8
GRB051221	328.703	16.891	53725.077	0.5468
GRB051210	330.171	-57.614	53714.241	2.5
GRB051117B	85.181	-19.274	53691.558	0.481
GRB051111	348.138	18.375	53685.25	1.5495
GRB051109	330.314	40.823	53683.05	2.346
GRB051022	359.017	19.607	53665.547	0.809
GRB051016B	132.116	13.656	53659.77	0.9364
GRB051008	202.873	42.098	53651.69	2.77
GRB051006	110.809	9.506	53649.855	1.059
GRB051001	350.953	-31.523	53644.466	2.4296
GRB050922C	317.388	-8.758	53635.83	2.198
GRB050922B	5.806	-5.605	53635.626	4.5
GRB050915	81.687	-28.016	53628.474	2.5273
GRB050908	20.461	-12.955	53621.238	3.347
GRB050904	13.711	14.085	53617.078	6.145
GRB050826	87.756	-2.643	53608.263	0.297
GRB050824	12.234	22.609	53606.967	0.83
GRB050822	51.113	-46.033	53604.159	1.434
GRB050820	337.409	19.560	53602.274	2.612
GRB050819	358.757	24.861	53601.683	2.5043
GRB050814	264.189	46.339	53596.485	5.535
GRB050803	350.658	5.786	53585.801	0.422
GRB050801	204.146	-21.928	53583.769	1.38
GRB050730	212.072	-3.772	53581.832	3.9678
GRB050724	246.185	-27.541	53575.524	0.2575
GRB050714B	169.699	-15.547	53565.945	2.4383

Name	RA (°)	decl (°)	TT (MJD)	z
GRB050709	345.362	-38.978	53560.942	0.16
GRB050603	39.987	-25.182	53524.27	2.821
GRB050525	278.136	26.339	53515.002	0.606
GRB050509B	189.058	28.984	53499.167	0.2255
GRB050505	141.764	30.273	53495.974	4.27
GRB050502B	142.542	16.997	53492.393	5.2
GRB050502	202.443	42.674	53492.093	3.793
GRB050416	188.478	21.057	53476.462	0.6535
GRB050408	180.573	10.852	53468.683	1.2357
GRB050401	247.870	2.187	53461.597	2.9
GRB050319	154.200	43.548	53448.397	3.24
GRB050318	49.713	-46.396	53447.656	1.44
GRB050315	306.476	-42.600	53444.875	1.949
GRB050223	271.385	-62.472	53424.131	0.5915
GRB050215B	174.448	40.797	53416.107	2.62
GRB050126	278.113	42.370	53396.501	1.29
GRB041219	6.108	62.083	53358.071	0.3
GRB041006	13.709	1.235	53284.512	0.716
GRB040924	31.594	16.114	53272.494	0.859
GRB040912	359.226	-1.001	53260.592	1.563
GRB031203	120.626	-39.850	52976.918	0.105
GRB030528	256.008	-22.650	52787.544	0.782
GRB030226	173.271	25.898	52696.157	1.986
GRB021211	122.270	6.678	52619.471	1.004
GRB021004	6.745	18.949	52551.504	2.33
GRB020903	342.176	-20.769	52520.421	0.25
GRB020819B	351.840	6.250	52505.623	1.9621
GRB020813	296.658	-19.588	52499.114	1.2545
GRB020405	209.513	-31.373	52369.029	0.69
GRB020127	123.756	36.776	52301.873	1.9
GRB020124	143.211	-11.520	52298.445	3.198
GRB011211	168.825	-21.949	52254.798	2.14
GRB011121	173.606	-76.028	52234.783	0.36
GRB010921	344.000	40.931	52173.219	0.45
GRB010222	223.052	43.018	51962.308	1.477
GRB000926	256.040	51.786	51813.877	2.066
GRB000911	34.681	7.741	51798.302	1.0585
GRB000418	186.330	20.103	51652.896	1.118
GRB000301C	245.078	29.443	51604.529	2.03
GRB000210	29.815	-40.659	51584.364	0.8463
GRB000131	93.262	-51.927	51574.624	4.5
GRB991216	77.380	11.285	51528.672	1.02
GRB991208	248.473	46.456	51520.192	0.706
GRB990712	337.971	-73.408	51371.323	0.434
GRB990705	77.477	-72.131	51364.668	0.842
GRB990510	204.525	-80.500	51308.367	1.619
GRB990506	178.671	-26.068	51304.475	1.3
GRB990123	231.374	44.758	51201.408	1.6
GRB980703	359.779	8.585	50997.182	0.966
GRB980613	154.442	71.486	50977.202	1.096
GRB980425	293.725	-52.819	50928.446	0.0085
GRB971214	179.110	65.200	50796.11	3.42
GRB970828	272.106	59.302	50688.739	0.9578
GRB970508	103.456	79.272	50576.904	0.835
GRB970228	75.488	11.768	50507.124	0.695

## Appendix B: GRB090401B, KM3-230213A and $\mathcal{S}_{dir}$

We here collect some information on 090401B and 230213A, focusing on what is relevant for the evaluation of  $\mathcal{S}_{dir}$  for the pair composed by 090401B and 230213A.

090401B is a long GRB ( $T_{90} = 183$  s), with measured redshift of 3.1 [18], whose J2000 coordinates are RA =  $95.088^\circ$ , decl =  $-8.972^\circ$  with an angular uncertainty of  $0.000065^\circ$  [15].

The J2000 coordinates of 230213A [14] are RA =  $94.3^\circ$ , decl =  $-7.8^\circ$  with containment radius  $R(68\%) = 1.5^\circ$ . (The available experimental information on the energy of 230213A is summarized in the main text.)

To characterize the level of directional agreement between 090401B and 230213A we use the statistic  $\mathcal{S}_{dir}$  given by  $\int P_{230213A}(\Omega)P_{090401B}(\Omega)d\Omega$ , where  $P_{230213A}(\Omega)$  and  $P_{090401B}(\Omega)$  are the angular distributions of 230213A and 090401B, respectively. For the evaluation of  $\mathcal{S}_{dir}$  we assumed that  $P_{230213A}(\Omega)$  and  $P_{090401B}(\Omega)$  are Gaussians characterized by the available experimental information on direction and directional uncertainty for 230213A and 090401B, finding that

$\mathcal{S}_{dir} = 194$ . Actually, because of the large difference in directional uncertainties, the angular distribution of 090401B can be approximated with a  $\delta$ -function when computing  $\mathcal{S}_{dir}$ .

## Appendix C: On the implications of a hypothetical sharper determination of the direction of 230213A

We here devote a small investigation to quantify the observation that in our assessment of the significance of the 090401B-230213A pair the uncertainty on the direction of 230213A is a key limitation.

For this purpose we replace the real directional uncertainty of 230213A, which is  $1.5^\circ$ , with  $0.2^\circ$ . The real 230213A has angular distance of  $1.4^\circ$  from the direction of 090401B, but for the purpose of this investigation we rescale this angular distance to  $0.187^\circ$ . The resulting value for our directional statistic would then be  $\mathcal{S}_{dir} = 10993$ . With these changes (and leaving all other aspects of the analysis unchanged) we redid the whole analysis, finding that in our hypothetical scenario a  $p$ -value of about 0.00024.

- 
- [1] G. Amelino-Camelia, J. R. Ellis, N. E. Mavromatos, D. V. Nanopoulos and S. Sarkar, *Nature* **393** (1998), 763.
- [2] J. Alfaro, H. A. Morales-Tecotl and L. F. Urrutia, *Phys. Rev. Lett.* **84** (2000), 2318.
- [3] A. Addazi *et al.*, *Prog. Part. Nucl. Phys.* **125** (2022), 103948.
- [4] M. Ackermann *et al.* [Fermi GBM/LAT], *Nature* **462** (2009), 331-334.
- [5] N. Aghanim *et al.* *Astron. Astrophys.* **641** (2020), A6 [erratum: *Astron. Astrophys.* **652** (2021), C4].
- [6] IceCube Collaboration, "IceCube HESE 12-year data release", <https://doi.org/10.7910/DVN/PZNO2T>, Harvard Dataverse, V2 (2023).
- [7] G. Amelino-Camelia, G. D'Amico, G. Rosati and N. Loreti, *Nature Astron.* **1** (2017), 0139.
- [8] Y. Huang and B. Q. Ma, *Communications Physics* **1** (2018), 62.
- [9] J. Ellis, N. E. Mavromatos, A. S. Sakharov and E. K. Sarkisyan-Grinbaum, *Phys. Lett. B* **789** (2019), 352-355.
- [10] G. Amelino-Camelia, M. G. Di Luca, G. Gubitosi, G. Rosati and G. D'Amico, *Nature Astron.* **7** (2023), 996.
- [11] G. Amelino-Camelia, G. D'Amico, V. D'Esposito, G. Fabiano, D. Frattulillo, G. Gubitosi, D. Guetta, A. Moia and G. Rosati, [arXiv:2501.13840 [gr-qc]].
- [12] U. Jacob and T. Piran, *Nature Phys.* **3** (2007), 87.
- [13] G. Amelino-Camelia, D. Guetta and T. Piran, *Astrophys. J.* **806** (2015), 269.
- [14] S. Aiello *et al.* [KM3NeT], *Nature* **638** (2025) no.8050, 376-382.
- [15] P. Schady and S. R. Oates, *GCN Circ.* 9067 (2009) 1.
- [16] P. Abbott *et al.* *Astrophys. J. Lett.* **848** (2017), L13.
- [17] M. G. Aartsen *et al.* *J. Phys. G* **48** (2021), 060501.
- [18] S. R. Oates *et al.*, *Mon. Not. Roy. Astron. Soc. Lett.* **426** (2012) Issue 1, L86-L90.